

LLNL-CONF-401127



LAWRENCE  
LIVERMORE  
NATIONAL  
LABORATORY

# Hydrocarbon-free resonance transition 795-nm rubidium laser

S. S. Q. Wu, T. F. Soules, R. H. Page, S. C. Mitchell, V. K. Kanz, R. J. Beach

February 7, 2008

Photonics West 2008  
San Jose, CA, United States  
January 21, 2008 through January 25, 2008

## **Disclaimer**

---

This document was prepared as an account of work sponsored by an agency of the United States government. Neither the United States government nor Lawrence Livermore National Security, LLC, nor any of their employees makes any warranty, expressed or implied, or assumes any legal liability or responsibility for the accuracy, completeness, or usefulness of any information, apparatus, product, or process disclosed, or represents that its use would not infringe privately owned rights. Reference herein to any specific commercial product, process, or service by trade name, trademark, manufacturer, or otherwise does not necessarily constitute or imply its endorsement, recommendation, or favoring by the United States government or Lawrence Livermore National Security, LLC. The views and opinions of authors expressed herein do not necessarily state or reflect those of the United States government or Lawrence Livermore National Security, LLC, and shall not be used for advertising or product endorsement purposes.

# Hydrocarbon-free resonance transition 795-nm rubidium laser

Sheldon S.Q. Wu,<sup>a,b</sup> Thomas F. Soules,<sup>a</sup> Ralph H. Page,<sup>a</sup> Scott C. Mitchell,<sup>a</sup> V. Keith Kanz,<sup>a</sup>  
Raymond J. Beach<sup>a</sup>

<sup>a</sup>Lawrence Livermore National Laboratory, 7000 East Avenue, Livermore, California 94551;

<sup>b</sup>Department of Electrical and Computer Engineering, University of California at San Diego, La Jolla, California 92093-0407

## ABSTRACT

An optical resonance transition rubidium laser ( $5^2P_{1/2} \rightarrow 5^2S_{1/2}$ ) is demonstrated with a hydrocarbon-free buffer gas. Prior demonstrations of alkali resonance transition lasers have used ethane as either the buffer gas or a buffer gas component to promote rapid fine-structure mixing. However, our experience suggests that the alkali vapor reacts with the ethane producing carbon as one of the reaction products. This degrades long term laser reliability. Our recent experimental results with a “clean” helium-only buffer gas system pumped by a Ti:sapphire laser demonstrate all the advantages of the original alkali laser system, but without the reliability issues associated with the use of ethane.

**Keywords:** rubidium laser, diode pumped alkali laser, DPAL

## 1. INTRODUCTION

The concept of an optically pumped alkali resonance laser was proposed by Konefal in 1999 [1]. Konefal’s proposal was for a longitudinally pumped alkali metal-molecular gas amplifier and was based on his experimental studies of collisionally induced fine-structure mixing in the presence of a molecular buffer gas such as ethane. Krupke extended Konefal’s laser proposal to include diode-pumping by introducing a buffer gas component such as He that would broaden the  $D_2$  transition making it more accommodating of diode pump array linewidths. The first experimental demonstration of an optically pumped alkali resonance laser occurred in 2002 at LLNL in which Rb vapor in a buffer gas mixture consisting of  $\sim 70$  Torr of ethane and  $\sim 500$  Torr of He was lased under pump excitation from a Ti:sapphire laser [2]. Since then, several demonstrations of alkali resonance transition lasers have been reported in the scientific literature using Rb [3], Cs [4, 5, 6] and K [7] as the gain media. A notable mention is the work done by Zhdanov *et al* which used extremely line-narrowed diode arrays,  $\Delta\lambda \approx 10$  GHz, to demonstrate 10 W class lasers with optical-optical efficiencies of  $>60\%$  in Cs [8]. Because they are compatible with commercially available laser diode pump sources and show promise for power scaling with good output beam quality, diode-pumped alkali lasers (DPAL) are being actively investigated today. Most reported demonstrations done to date have used ethane as the buffer gas or a buffer gas component in the alkali vapor cell. This approach uses ethane to promote rapid fine-structure mixing, a requirement for efficient laser operation, between the terminal pump level ( $^2P_{3/2}$ ) and the initial laser level ( $^2P_{1/2}$ ). One issue with this approach is the chemical reaction that takes place between the alkali and the ethane. Although the deposition of carbon can be a slow process and may not impact experiments over several hours of run time, the problem developed in all of our cells eventually, especially higher temperature cells ( $T > 135^\circ\text{C}$ ) as reported by Page *et al* [3]. Here we report experimental demonstration of the first Rb optical resonance transition laser using a pure He buffer gas. Our experimental results are compared with model predictions and support the use of a clean, hydrocarbon-free Rb-He system for power scaling.

Rb has two dominant optical transitions, commonly referred to as the  $D_1$  and  $D_2$  lines. The two lines are located at 795 and 780 nm respectively and can be easily accessed by a variety of light sources including commercially available laser diode arrays. Optical gain is achieved by pumping on the  $D_2$  ( $5^2S_{1/2} \rightarrow 5^2P_{3/2}$ ) transition and extracting on the  $D_1$  ( $5^2P_{1/2} \rightarrow 5^2S_{1/2}$ ) transition. While the  $D_1$  and  $D_2$  transitions are electric dipole transitions and possess large emission cross sections, the  $5^2P_{3/2} \rightarrow 5^2P_{1/2}$  transition is not. Inelastic collisions with buffer gas atoms can provide the population transfer needed to reach inversion. Hence, to facilitate fast transfer of population between the fine-structure levels, a buffer gas is commonly added to the system. Fig 1 shows the Rb energy levels of interest.

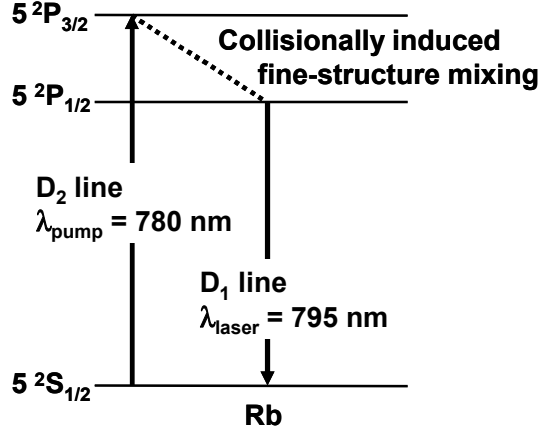


Fig. 1. Rb energy level diagram. Optical gain is achieved by pumping on the D<sub>2</sub> transition and extracting on the D<sub>1</sub> transition.

Ethane possesses a large Rb fine-structure mixing cross section and has been used in most reported demonstrations to effectively mix the upper states. However, one issue with this approach is the chemical reaction that takes place between the alkali and the ethane. The chemical reaction,  $6X + C_2H_6 \rightarrow 6XH + 2C$  (graphite), where X is the alkali (K, Rb, or Cs) and XH is the corresponding hydride, is thermodynamically favored and has a large negative free energy [9]. In our previous experiments that had used ethane as a component of the buffer gas, we observed that carbonaceous deposits formed at cell surfaces (e.g. windows) that simultaneously saw high intensity pump light and were exposed to alkali vapor and ethane. This negative effect was observed in other reported demonstrations as well [8]. Because we are ultimately interested in using end-pump geometries in which high intensity pump light is ducted through a cell via reflections with the side walls of the cell where pump light, ethane and alkali vapor meet together, it is essential that we mitigate this problem for reliable power scaling. While the predicted optical to optical efficiencies of >60% have been demonstrated by workers in the field, confirming the anticipated scalability of alkali lasers, the issue of cell degradation has not been resolved. Helium, a gas commonly used to broaden the alkali transition lines, has been shown to possess some of the desirable properties of ethane but without the highly undesirable reactions. Beach *et al* calculated that the Rb-He fine-structure mixing cross section is sufficient to permit efficient diode-pumped Rb based systems at He buffer gas pressures of ~10 atm and higher [4]. Obviated is the issue of carbon formation and degradation of the vapor cell that we observed in our previous alkali laser demonstrations that used ethane as a buffer gas component to promote rapid fine-structure mixing.

Extended laser modeling was conducted following the formalism outlined in Ref [4] and summarized below. The model is based on a master equation approach in the rate equation approximation. Longitudinal averaging is used to simplify calculations without loss of applicability to high gain laser media. In the equations,  $n_1$  represents the population in the ground state ( $5^2S_{1/2}$ ), and  $n_2$  and  $n_3$  represent the populations in  $5^2P_{1/2}$  and  $5^2P_{3/2}$  states respectively. Collision induced excitation transfer rate between the fine-structure levels is represented by  $\gamma$ 's. Quenching collision transfer rates to the ground state are negligibly small in the case of He and need not to be considered in these calculations. The equations that govern the distribution of populations in the laser are

$$\begin{aligned}
 \frac{dn_3}{dt} &= \Gamma_P - \gamma_{2P_{3/2} \rightarrow 2P_{1/2}} n_3 + \gamma_{2P_{1/2} \rightarrow 2P_{3/2}} n_2 - \frac{n_3}{\tau_{D_2}} \\
 \frac{dn_2}{dt} &= -\Gamma_L + \gamma_{2P_{3/2} \rightarrow 2P_{1/2}} n_3 - \gamma_{2P_{1/2} \rightarrow 2P_{3/2}} n_2 - \frac{n_2}{\tau_{D_1}} \\
 \frac{dn_1}{dt} &= -\Gamma_P + \Gamma_L + \frac{n_2}{\tau_{D_1}} + \frac{n_3}{\tau_{D_2}}
 \end{aligned} \tag{1}$$

where  $\Gamma_P$  and  $\Gamma_L$  are the transition rates associated with pump photon absorption and laser photon emission respectively. We do not assume that local thermal equilibrium exists *a priori* between the  $5^2P_{1/2}$  and the  $5^2P_{3/2}$  levels because of the

limited Rb-He fine structure mixing rate and continue to carry the full set of rate equations in our modeling of the alkali system. The appropriate expressions for  $\Gamma_p$  and  $\Gamma_L$  are

$$\Gamma_p = \frac{\eta_{mode}\eta_{del}}{V_L} \int d\lambda \frac{P_{pump}(\lambda)}{hc/\lambda} \left[ 1 - e^{-\left(n_1 - \frac{1}{2}n_3\right)\sigma_{D_2}(\lambda)l} \right] \left[ 1 + R_p e^{-\left(n_1 - \frac{1}{2}n_3\right)\sigma_{D_2}(\lambda)l} \right] \quad (2)$$

$$\Gamma_L = \frac{1}{V_L} \frac{P_{laser}}{hc/\lambda_{D1}} \frac{R_{OC}}{1-R_{OC}} T_{window} \left( \frac{1}{T_{window}^2 \sqrt{R_{OC}R_{HR}}} - 1 \right) \left( 1 + \sqrt{\frac{R_{HR}}{R_{OC}}} \right)$$

where  $V_L$  is the volume of the laser mode,  $\eta_{mode}$  is the fraction of the pump light that intercepts the laser mode's cross-sectional area and thus contributes to lasing,  $\eta_{del}$  is the fraction of the pump power delivered from the pump excitation source to the input of the laser gain medium,  $P_{pump}(\lambda)$  is the spectrally resolved pump power,  $R_p$  represents the reflectivity of the pump light on the high reflecting mirror after single passing the laser gain medium,  $\sigma_{D_2}(\lambda)$  is the spectrally resolved pump absorption cross section,  $T_{window}$  is the transmission efficiency through a single cell window. All mixing rates, lifetimes, broadening rates, and cross sections are taken from published scientific literature.

Based on our model predictions, the lack of ethane induced mixing of the Rb fine-structure levels can be sufficiently overcome by a higher density of He. Due to the small spectral linewidth of the pump source used for this demonstration, population inversion between the lasing levels can be attained at He pressures of a few atmospheres. We project that in diode-pumped power scaled systems, optical to optical efficiencies of  $>70\%$  can be reached with the same hydrocarbon-free approach using conventional diode arrays. The use of atmospheres of He as the buffer gas is compatible with pump linewidths of  $\sim 0.5\text{nm}$ , a regime requiring only modest linewidth control with today's conventional 2-d stacks of laser diode array technology. Hydrocarbon-free diode-pumped alkali lasers present a new pathway to high average power with good beam quality and high efficiency.

## 2. EXPERIMENT

A schematic diagram for the experimental setup used to demonstrate the hydrocarbon-free Rb laser is shown in Fig. 2. The Rb vapor and He gas were contained in a 3 cm long cylindrical ceramic cell with sapphire windows that were AR coated on their external surfaces, but uncoated on their internal surfaces. Rb was introduced into the cell as a pure metal. This was followed by cell evacuation using a laboratory vacuum system and then the introduction of 40 psi of He gas (2.7 atm) at room temperature ( $\sim 20^\circ\text{C}$ ). The cell was placed in a close-fit copper oven with electric heaters that allowed us to maintain the cell temperature to within  $1^\circ\text{C}$  and to fix the resulting Rb saturated vapor pressure inside the cell. The entire cell was heated to temperatures up to  $170^\circ\text{C}$ , corresponding to a Rb vapor density of  $2.2 \times 10^{14} \text{ cm}^{-3}$  inside the cell.

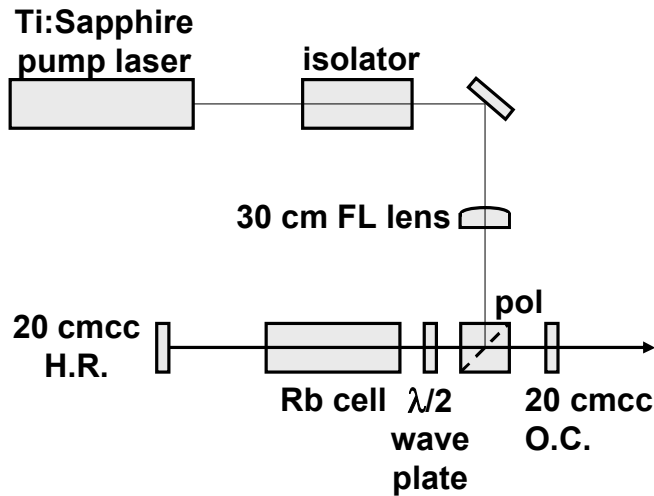


Fig. 2. Schematic diagram of the experimental setup used in our demonstrations. The laser cavity mirrors have  $\sim 20$  cm radii of curvature and are both concave (cc). H.R. stands for high reflector, O.C. for output coupler and FL for focal length.

The pump source used was a Ti:sapphire laser that produced up to 2.7 W of linearly polarized, near-diffraction-limited CW optical radiation. The Ti:sapphire laser linewidth was  $\sim 9$  GHz FWHM making the pump laser source narrow compared to the He-broadened  $D_2$  pump absorption feature, which we estimate is  $\sim 50$  GHz wide based on the known Rb-He collisional broadening rate of 18.1 GHz/amagat [10]. The pump light was coupled into the 40.5 cm long laser cavity via a polarizing beam splitter and traversed the vapor cell twice by reflecting off the highly reflecting end mirror. The end mirror has about 0.99 reflectivity at both the pump and lasing wavelengths. The pump beam was aligned parallel to the laser cavity axis and focused to a  $220 \mu\text{m}$  diameter spot size at the center of the cell, resulting in peak pump irradiances of nearly  $5 \text{ kW/cm}^2$ . Since the optic axes of the pair of sapphire windows were set at unknown orientations, a half-wave plate was placed in the cavity to partially compensate for the polarization changes caused by birefringence. We estimate that even with the half-wave plate, laser light traversing the cell had a 75% transmission efficiency passing the cube polarizer on its return path.

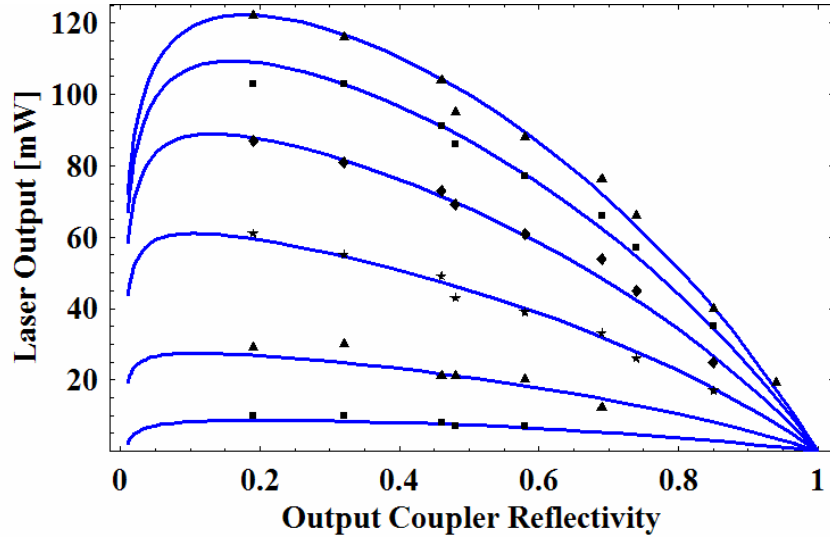


Fig. 3. Rb laser output power for various pump powers plotted against output coupler reflectivity. Solid curves represent model predictions. From top to bottom, pump powers are: 1.81W, 1.53W, 1.23W, 0.93W, 0.63W, 0.47W.

We successfully observed linearly polarized CW laser emission at 795 nm in a  $TEM_{00}$  beam at cell temperatures in the vicinity of  $145^\circ\text{C}$ . Maximum powers of over 130 mW and optical to optical efficiencies close to 7% were measured despite single-pass passive optical losses near 40% in our laser cavity from cube polarizer and window reflections. Presented in Fig. 3 is the theoretical and measured laser output power versus output coupler reflectivity at several Ti:sapphire pump laser powers. The reflectivities of the output couplers were directly measured using a Ti:Sapphire probe beam at 795 nm. The reported pump powers were measured outside the laser cavity and delivered into the laser cavity with an efficiency of 0.9. Large cavity losses along with the high gains that characterize alkali atoms put the optimal output coupler reflectivity at below 0.2. These high values for optimized output coupling support the use of geometrically unstable resonators for the scaling of diode-pumped alkali lasers to high power with good beam quality. The theoretical curves overlaying the experimental data points were calculated using a laser model previously developed by Beach *et al* [4]. Using experimentally measured values and treating the beam overlap and the Rb-He fine-structure mixing rate as adjustable parameters, we were able to find excellent agreement between our model and laser output data. The model curves were generated using an effective Rb-He fine-structure mixing cross section value of  $4.6 \times 10^{-17} \text{ cm}^2$  and 24% mode overlap efficiency. Mode overlap is defined as in [4] as the fraction of the pump excited volume in the alkali cell extracted by the circulating laser radiation in the resonator. We attribute the low overlap efficiency to a mismatch between the pump and laser beam waists at the cell center, the pump laser beam waist (1/e-HW) being measured to be  $110 \mu\text{m}$  and the laser mode beam waist estimated to be  $75 \mu\text{m}$  at cell center, and our inability to get perfect collinear overlap of the pump and the laser beams through the length of the 3 cm long cell. We note the Rb-He fine-structure mixing rate that gave the best fit between our model and experimental data is approximately three times larger than that predicted based on cross sections previously reported by Gallagher [11]. Fig. 4 shows a plot of

measured laser output power against cell temperature, acquired as the cell temperature was continuously varied between 115 and 160°C. For this data the output coupler had a measured reflectivity of 0.19. The model parameter values used to generate the model overlay of the data in Fig. 4 are the same as those used for the overlay shown in Fig. 3.

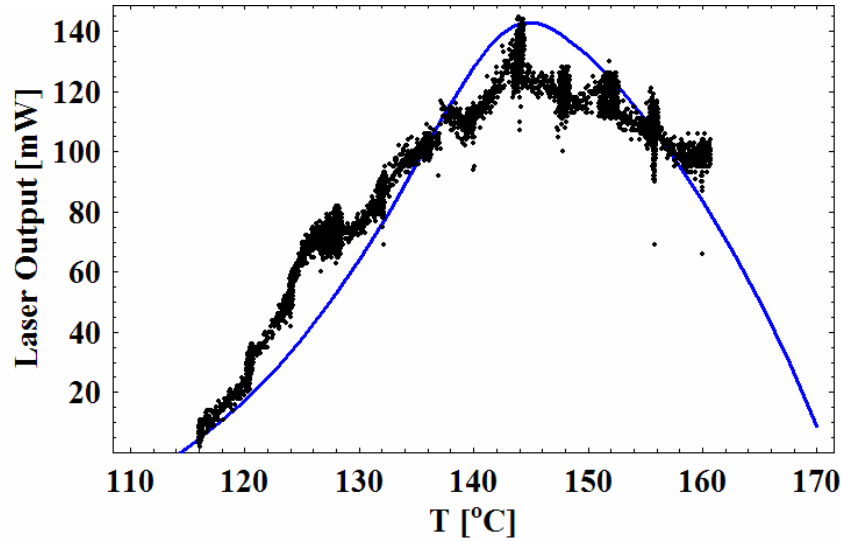


Fig. 4. Rb laser output power with varying cell temperature using a 0.19 reflectivity output coupler. Solid curve shows model prediction.

Fig. 5 is a different plot of the data from Fig. 3 illustrating a feature of the Rb laser using pure He buffer gas. Both our data and the overlaid laser model predict a decrease or roll off in slope efficiency at higher pump powers. This decrease in slope efficiency is caused by the limited mixing rates between the Rb fine-structure energy levels. After a Rb atom is optically excited to  $5^2P_{3/2}$  energy level, it radiatively returns to the  $5^2S_{1/2}$  ground level or transfers its energy via He collision to the  $5^2P_{1/2}$  initial laser level. Under strong pumping, the limited fine-structure mixing rate is insufficient in keeping the initial laser level appropriately filled for optimum laser operation, *i.e.* the initial laser level is essentially starved for population at the higher pump excitation rates resulting in the observed roll off in slope efficiency. For this demonstration of the hydrocarbon-free rubidium laser, we purposely picked operating conditions suitable for the Ti:sapphire pump laser that also present a slight bottleneck in laser performance. Agreement between model and experiment supports our understanding of the underlying physical processes. We note here that this saturation behavior is expected to be negligible for power scaled diode pumped systems which operate at significantly higher He pressures.

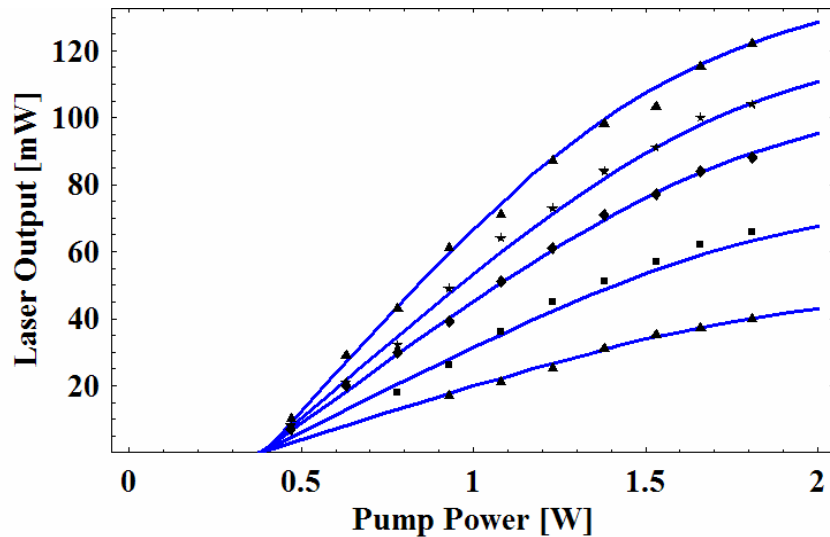


Fig. 5. Rb laser output power for various output couplers plotted against pump power. Solid curves represent model predictions. From top to bottom, the reflectivities are: 0.19, 0.46, 0.58, 0.74, 0.85.

The same clean, hydrocarbon-free approach being reported here for Rb based systems is also applicable for K-based systems, but not Cs-based systems. This is because the Cs-He fine-structure mixing cross section is too small to make a He-only buffer gas system feasible using Cs. The reported value for the Cs-He fine structure mixing cross section is almost three orders of magnitude smaller than the Rb-He cross section value [11].

### 3. CONCLUSIONS

In summary, the first hydrocarbon-free optical resonance transition rubidium laser has been demonstrated. Good agreement between measured laser performance and our laser model supports further pursuing this approach for power scaling. Obviated is the issue of carbon formation and degradation of the vapor cell that we observed in our previous alkali laser demonstrations that used ethane as a buffer gas component to promote rapid fine-structure mixing. We have been able to reuse the cell for multiple (>8) heating cycles and three helium fills without any signs of degradation. Because of its model projected efficiency advantages over diode-pumped solid state lasers (DPSSLs), its compatibility with commercially available laser diode arrays, and now a demonstrated system that promise very high reliability, diode-pumped He-only Rb lasers will potentially compete favorably with DPSSLs in many applications that require high beam quality CW or quasi-CW laser operation.

We are grateful to Prof. Paul Yu of UC San Diego; John O'Pray, Mike Tobin, Kevin Zondervan, Jim Kotora, Denise Podolski, Mark Rotter, all of the Missile Defense Agency, Jeff Thomas, Eliot Geathers, Tom Leheka, Brian Brickeen, Dave Bernot, all of the Penn State Electro Optics Center, and Chris Barty of Lawrence Livermore National Laboratory for their support and many useful discussions. We also gratefully acknowledge the financial support provided by the Missile Defense Agency and the Penn State Electro Optics Center for the work reported within. This work performed under the auspices of the U.S. Department of Energy by Lawrence Livermore National Laboratory under Contract DE-AC52-07NA27344.

#### References

- <sup>1</sup> Z. Konefal, "Observation of collision induced processes in rubidium-ethane vapour", *Opt. Com.* 164, 95-105 (1999).
- <sup>2</sup> W. F. Krupke, R. J. Beach, V. K. Kanz, and S. A. Payne, "Resonance transition 795-nm rubidium laser," *Opt. Lett.* 28, 2336-2338 (2003).
- <sup>3</sup> R. H. Page, R. J. Beach, V. K. Kanz, and W. F. Krupke, "Multimode-diode-pumped gas (alkali-vapor) laser," *Opt. Lett.* 31, 353-355 (2006)
- <sup>4</sup> R. J. Beach, W. F. Krupke, V. K. Kanz, S. A. Payne, M. A. Dubinskii, and L. O. Merkle, "End-pumped continuous-wave alkali vapor lasers: experiment, model, and power scaling," *J. Opt. Soc. Am. B* 21, 2151-2163 (2004).
- <sup>5</sup> T. Ehrenreich, B. Zhdanov, T. Takekoshi, S. P. Phipps, and R. J. Knize, "Diode Pumped Cesium Laser", *Electronics Lett.* 41, 47-48 (2005).
- <sup>6</sup> Y. Wang, T. Kasamatsu, Y. Zheng, H. Miyajima, H. Fukuoka, S. Matsuoka, M. Niigaki, H. Kubomura, T. Hiruma, H. Kan, "Cesium vapor laser pumped by a volume-Bragg-grating coupled quasi-continuous-wave laser-diode array", *Appl. Phys. Lett.* 88, 141112 (2006).
- <sup>7</sup> B. Zhdanov, C. Maes, T. Ehrenreich, A. Havko, N. Koval, T. Meeker, B. Worker, B. Flusche and R. J. Knize, "Optically Pumped Potassium Laser", *Opt. Com.* 270, 353-355 (2007).
- <sup>8</sup> B. Zhdanov and R. J. Knize, "Diode-pumped 10 W continuous wave cesium laser," *Opt. Lett.* 32, 2167-2169 (2007)
- <sup>9</sup> FactSage 5.5<sup>TM</sup> / FactWeb<sup>TM</sup>, CRCT, Ecole Polytechnique, Montreal, Canada, (2007).
- <sup>10</sup> M. V. Romalis, E. Miron, and G. D. Gates, "Pressure broadening of Rb D<sub>1</sub> and D<sub>2</sub> lines by <sup>3</sup>He, <sup>4</sup>He, N<sub>2</sub>, and Xe: Line cores and near wings", *Phys. Rev. A* 56, 4569-4578 (1997).
- <sup>11</sup> A. Gallagher, "Rubidium and Cesium Excitation Transfer in Nearly Adiabatic Collisions with Inert Gases", *Phys. Rev.* 172, 88 (1968)